Molecular dynamics simulations of stretched gold nanowires: The relative utility of different semiempirical potentials

Qing Pu and Yongsheng Leng[a)]
Department of Chemical Engineering, Vanderbilt University, Nashville, Tennessee 37235

Leonidas Tsetseris
Department of Physics and Astronomy, Vanderbilt University, Nashville, Tennessee 37235

Harold S. Park
Department of Civil & Environmental Engineering, Vanderbilt University, Nashville, Tennessee 37235

Sokrates T. Pantelides
Department of Physics and Astronomy, Vanderbilt University, Nashville, Tennessee 37235 and Materials Science and Technology Division, Oak Ridge National Laboratory, Oak Ridge, Tennessee 37831

Peter T. Cummings
Department of Chemical Engineering, Vanderbilt University, Nashville, Tennessee 37235 and Nanomaterials Theory Institute, Center for Nanophase Materials Sciences, Oak Ridge National Laboratory, Oak Ridge, Tennessee 37831

(Received 15 August 2006; accepted 21 February 2007; published online 12 April 2007)

The mechanical elongation of a finite gold nanowire has been studied by molecular dynamics simulations using different semiempirical potentials for transition metals. These potentials have been widely used to study the mechanical properties of finite metal clusters. Combining with density functional theory calculations along several atomic-configuration trajectories predicted by different semiempirical potentials, the authors conclude that the second-moment approximation of the tight-binding scheme (TB-SMA) potential is the most suitable one to describe the energetics of finite Au clusters. They find that for the selected geometries of Au wires studied in this work, the ductile elongation of Au nanowires along the [001] direction predicted by the TB-SMA potential is largely independent of temperature in the range of 0.01–298 K. The elongation leads to the formation of monatomic chains, as has been observed experimentally. The calculated force-versus-elongation curve is remarkably consistent with available experimental results. © *2007 American Institute of Physics*. [DOI: 10.1063/1.2717162]

I. INTRODUCTION

The molecular break-junction technique is a method for preparing configurations of metallic electrodes linked through a single molecule. In particular, organic molecules bonded between two gold electrodes have emerged as prototypical metal-molecule-metal configurations in molecular electronic devices, and their current-voltage (*I-V*) characteristics have attracted considerable interest in both experiments[1–3] and theories.[4–8] In addition to the relevance of the break-junction technique for the study of molecular electronic devices, pulling a notched gold wire apart is in itself an interesting physical process. For this reason, the formation of Au nanowires has been studied extensively with a number of experimental techniques, such as scanning tunneling microscopy (STM),[9–11] atomic force microscopy,[12,13] mechanically controllable break junction,[14,15] and *in situ* high resolution transmission electron microscopy.[11,16–18] On the theoretical side, simulations have provided atomic-scale details of the chain formation, particularly on the final stages before the gold chains break apart.[17,19–21] The elongation process has been modeled using molecular dynamics (MD) simulations with either empirical potentials [for example, using the glue model,[22] the effective medium theory potential,[21] Sutton-Chen potential,[23] and the embedded-atom method (EAM) potential[24]] that aim to take into account many-body effects, or using potentials which are calibrated to reproduce features of the band structure through the second moment of density of state [for example, the second-moment approximation of the tight-binding scheme[25] (TB-SMA) and Finnis-Sinclair potential[26,27]]. Approaches that include the electronic structure explicitly are also available through first-principles quantum mechanical calculations.[19,28–31] Whereas such techniques can provide parameter-free results, they are inherently limited to systems of small size and to a small number of configurations, usually those corresponding to the final stages before breakup or the selected parts of the Au tip-neck-tip system.[28,30] Semiempirical potentials have lesser accuracy but can handle very large systems with relatively low computational cost. However, semiempirical potentials are usually constructed for and tested on bulk systems, where all atoms have full or near-full coordination. In some cases, the potentials are optimized to

[a)]Author to whom correspondence should be addressed. Electronic mail: yongsheng.leng@vanderbilt.edu

handle surfaces. Thus, potentials calibrated using bulk and infinite-surface properties may or may not work well for the very low-coordinated atomic chains. A comparison using the same protocol for different approaches would be valuable. In this respect, first-principles methods are ideal for evaluating the semiempirical potentials, with the aim of establishing an optimal simulation approach for nanostructures with large numbers of low-coordination atoms.

In this paper, we combine MD simulations with density functional theory (DFT) calculations to evaluate the quality of typical empirical or semiempirical potentials widely used in the MD simulation community. The test system is a finite gold cluster under elongation along [001] direction. Three different force fields, the glue model,[32] the EAM,[33] and the TB-SMA,[25] have been used in MD simulations. We found that the TB-SMA potential is the most suitable one to describe the elongation properties of gold nanowire. Using this approach, we further investigate the temperature effect on the elongation property of gold nanowires for the selected systems. We find that for (001) Au nanowire, the elongation ductility is independent of temperature in the range of 0.01–298 K, which may be due to the specific geometries studied here. This result is in contrast to results of prior simulations based on empirical or semiempirical potentials,[34] but no experimental evidence is available for comparison, leaving an open question for future studies. Our calculations further illustrate that the TB-SMA potential can correctly predict the breaking force (1.5 nN) of the monatomic chains in the final stage of breakup, as observed in experimental measurement.[30]

II. SIMULATION METHOD

We focus on three semiempirical force fields: the glue model potential proposed by Ercolessi *et al.*,[32] the EAM (Refs. 33 and 35) originally developed by Daw and Baskes,[36] and the TB-SMA developed by Cleri and Rosato.[25] Though all of these three potentials include many-body effects, which are very important for the metallic bonding in transition metal systems, their derivations are quite different. The glue model is a purely empirical potential whose parameters are fitted to important thermal and surface properties of the system of interest.[32] The EAM potential is a semiempirical potential that allows for electron density variations depending on the local bonding environment. The TB-SMA potential has been derived based on a different scheme that includes the long-range band-structure effects.[25]

We have performed MD simulations for the elongation of Au nanowires along the [001] direction at two typical temperatures, 0.01 and 298 K. Two system sizes have been considered. For the small system, the Au nanowire contains 16 layers of gold with a total of 256 atoms [see Fig. 1(a)]. Before pulling, the system is allowed to relax for 120 ps. For the large system, the Au nanowire has 32 layers of gold containing 3254 atoms [see Fig. 2(a)]. The notched wire in this case is to aid the breakup at the central part of the wire. In both systems, the last two layers at each end are kept rigid, and all the other atoms are dynamic. Elongation is conducted by pulling the top rigid layers along the z direction (i.e., the [001] direction) with an increment of 0.1 Å, while keeping the other end fixed. For every 0.1 Å increment, the whole system is allowed to be fully relaxed for 5000 time steps with a time step of 2 fs. We carefully examined the relaxation process of 256 Au wire at 0.01 K and concluded that this relaxation time is sufficient to relax any energy bumps due to the sudden 0.1 Å jumps of the top rigid layers. The equations of motion are integrated via the velocity Verlet algorithm and the temperature is controlled by Nosé-Hoover thermostat.[37–39]

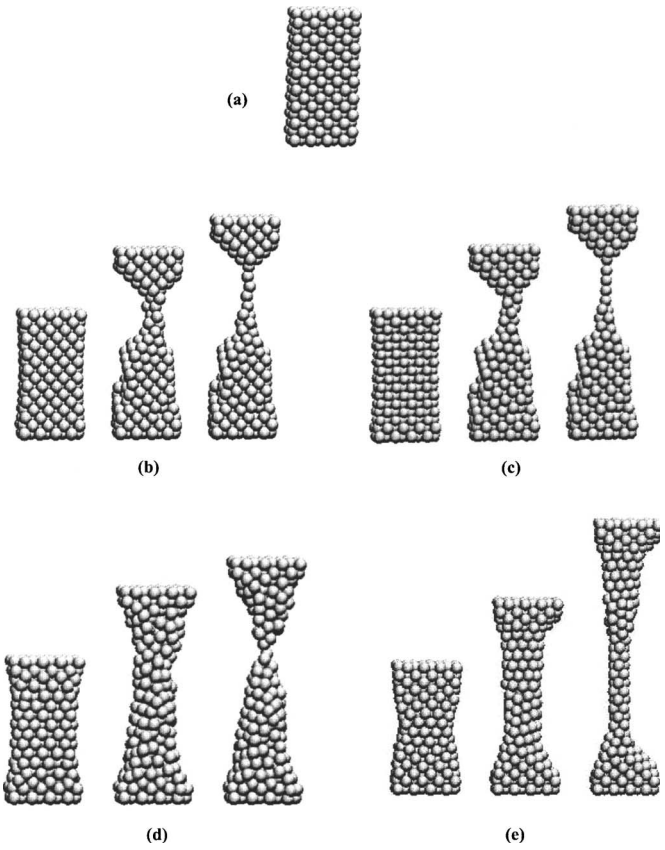

FIG. 1. Representative snapshots for the elongation process of small Au (001) system at 0.01 K: (a) initial unrelaxed bulk structure; (b) DFT relaxed configurations prior to pulling, the intermediate stage (1590 ps), and the final break junction (2390 ps) along TB-SMA trajectory; (c) the TB-SMA configurations prior to pulling, the intermediate stage (1590 ps), and the final break junction (2390 ps); (d) the glue model configurations prior to pulling, the intermediate stage (1590 ps), and the break junction (2208 ps); and (e) the EAM configurations prior to pulling, the intermediate stage (1590 ps), and the final break junction (3570 ps).

The DFT calculations for the 256-atom small Au nano-

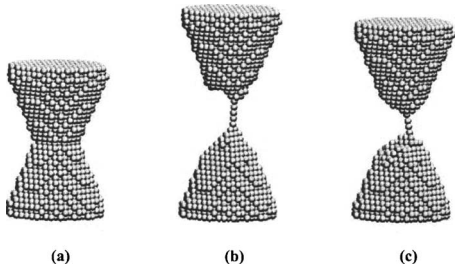

FIG. 2. The atomic configurations of the large Au (001) nanowire: (a) the initial configuration, (b) the break-junction structure at 0.01 K, and (c) the break-junction structure at 298 K.

TABLE I. The energy drops ΔE (kcal/mol) from the DFT energy calculation and the other three force field predictions. ($\Delta E = E_{\text{crystal}} - E_{\text{relaxed}}$)

	DFT	TB-SMA	Glue	EAM
ΔE	185.93	186.91	1369.28	705.44

wire use a local-density approximation (LDA) exchange-correlation functional,[40] ultrasoft pseudopotentials,[41] and a plane-wave basis as implemented in the VASP code.[42] We use Γ point sampling and an energy cutoff of 180 eV. Tests using an energy cutoff of 240 eV resulted in insignificant changes in the results quoted here. LDA functional is known to describe accurately[43,44] both bulk and surface properties of Au.

III. RESULTS AND DISCUSSION

A. Static structure relaxation

We first study the static structure relaxation of a 256-atom gold cluster from an initially unrelaxed configuration, corresponding to the bulk crystal, as shown in Fig. 1(a). The "energy drops," defined as the energy differences between the relaxed and unrelaxed configurations at $T=0.01$ K, are summarized in Table I. We see that the TB-SMA energy drop has almost the same value as that given by the DFT calculation. In comparison, both the glue model and the EAM potential yield energy drops that are noticeably larger. In particular, the energy drop given by the glue model is almost eight times of the DFT result. This over-relaxation by the glue and EAM potentials can be also seen clearly in Figs. 1(d) and 1(e), respectively, the relaxed configurations prior to pulling. In contrast, Figs. 1(b) and 1(c) show that both the DFT and the TB-SMA potentials give almost the same relaxed atomic configurations.

B. Dynamic elongation behavior

We now explore the elongation behavior of the small gold nanowire. The three semiempirical potentials generate three different elongation-energy paths. Along these three different atomic-configuration trajectories, DFT total energy calculations are performed. The relative elongation-energy differences between the DFT results and the corresponding results predicted by the different potentials are shown in Fig. 3(a). In this figure, the total energies of the initial *unrelaxed* configuration (the bulk crystal, E_{crystal} given either by the DFT or semiempirical potentials are taken as the initial reference points. Evidently, the minimum elongation-energy difference curve between the MD and the DFT calculations corresponds to that given by the TB-SMA potential. Figure 3(b) enlarges a part of Fig. 3(a) to clearly show the energy differences between the TB-SMA and the DFT results with different energy cutoff. The relative elongation-energy differences between the DFT and the other two MD simulation results given by the glue and EAM, as clearly shown in the figure, are dramatic. This is particularly true for the glue model.

The initial, intermediate, and final break-junction atomic configurations given by the three semiempirical potentials are shown in Figs. 1(c)–1(e). The total elongations at T

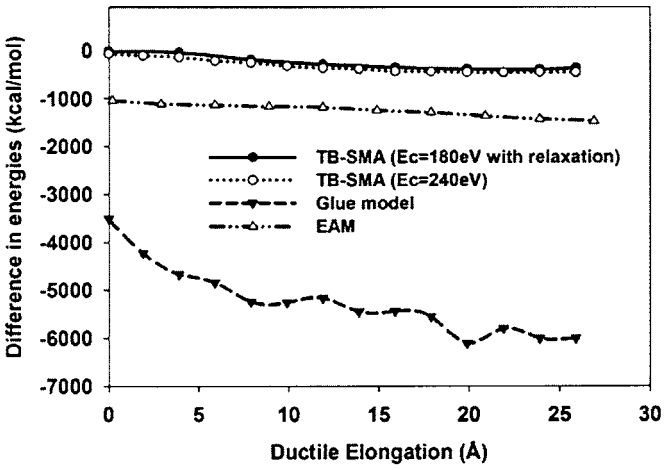

(a)

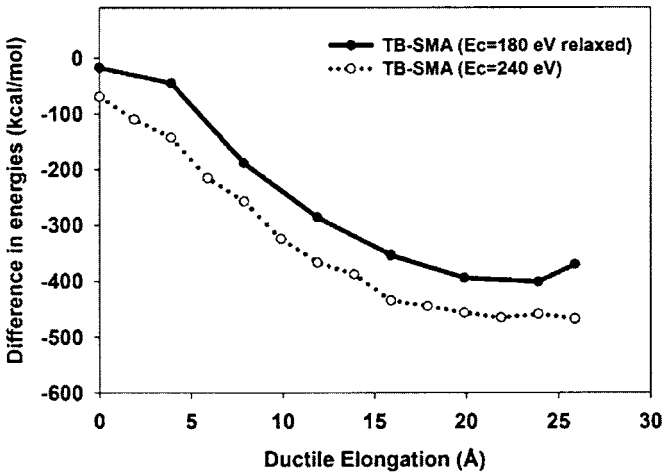

(b)

FIG. 3. (a) The relative elongation-energy differences between the results given by the semiempirical potentials and by the DFT calculations for small Au (001) system at 0.01 K. This relative elongation-energy difference is defined as $\Delta E = [E(t) - E_{\text{crystal}}]_{\text{classic}} - [E(t) - E_{\text{crystal}}]_{\text{DFT}}$. (b) The enlarged diagram for the results along the TB-SMA trajectory. Along the TB-SMA trajectory, the complete DFT energy relaxation calculation (energy cutoff =180 eV) gives a relatively lower energy difference (solid line), as compared with the total DFT energy calculation with an even higher energy cutoff of 240 eV (dotted line). (DFT energy calculation with an energy cutoff of 180 eV yields almost the same result as that of 240 eV cutoff, thus demonstrating the convergence of the DFT results relative to the energy cutoff of the basis set.)

$=0.01$ K before breakup are 24.9, 22.0, and 35.7 Å, respectively, for the TB-SMA, the glue model, and the EAM potentials. Obviously, the EAM gives a much longer ductile elongation.

The comparably small energy differences between the DFT and the TB-SMA results suggest that the TB-SMA potential favors the formation of low energy break-junction structures, whereas the glue model and the EAM potential yield relatively higher energy structures. This indicates that the glue and the EAM models are not suitable for low-coordinated systems such as Au ultrathin chains, though *all* the three semiempirical potentials are calibrated to the bulk

properties. The formation of monatomic chain structures found by the TB-SMA simulations, which is inherently a quantum phenomenon, has been observed in several experimental studies.[11,17,18] The ability of the TB-SMA potential to simulate the experimentally observed monatomic chain structure is probably due to the fact that it has been constructed based on the underlying electronic band structure and relatively longer range cutoff,[25] which is likely to be an essential feature in describing the dynamical formation of thin wires, particularly in the last stage of the formation of monatomic chains.

Our further investigations on the mechanical elongation of gold nanowires using the TB-SMA potential revealed other interesting phenomena. One of the fundamental question concerns the thermal effect on the elongation property. For this reason, we have performed four sets of MD runs that include small (256 Au atoms) and large (3254 Au atoms) systems at low (0.01 K) and room temperature (298 K). Each set contains 30 independent MD runs starting from different initial equilibrium configurations. For the small system (256 Au atoms) at 298 K, we find that in most cases, only one or two Au monatomic chains are formed [see Fig. 4(a)]. Interestingly, the average elongation at the breakup point is 18.64±4.2 Å, which is insignificant when compared with the elongation at $T=0.01$ K, i.e., 18.82±2.1 Å. For the large system with a notched shape, monatomic chains at $T=0.01$ and 298 K are observed, as shown in Figs. 2(b) and 2(c), respectively. The independent MD runs (30 MD runs for each temperature) show that the average elongations at 0.01 and 298 K are 16.5±2.4 and 16.7±2.7 Å, respectively. The lesser elongation at breakup for the large system, compared with the small system, is probably due to the notched shape of the gold wires that aids the early breakup and may also attribute to the smaller probability of the monatomic chains formed in the statistical study. We postulate that the similarity in elongations for the same size nanowire between the results at 0.01 and 298 K is primarily due to the fact that at 298 K Au nanowire is well below its melting point (e.g., for a 256-atom Au nanowire, our preliminary simulations suggest that the melting point is ~550 K,[45] while for a 3254-atom Au nanowire, the melting point would be considerably higher), and the failure modes at the two temperatures are essentially the same, i.e., the final elongation largely depends on the local fracture strain. It may also be due to the specific constrained geometries of gold nanowires studied in this work, in which the thermal oscillation along the elongation direction is hindered by the fixed boundaries. Further investigations are needed to explore more general cases including the length effect and thermal vibrations[46] on the elongation property of gold nanowires.

The TB-SMA prediction on the temperature independence of elongation of Au (001) nanowire contrasts to the result reported in other MD studies for Cu (001) nanowires using the EAM potential that found a temperature dependence.[34] We found the similar temperature dependence of Au (001) nanowire when using the EAM for small Au nanowire, as shown in our present study in Fig. 4, in which the EAM potential predicts a much longer Au thick neck before breakup. As shown in Figs. 4(b) and 4(c), both the glue and EAM potentials generate much longer and thicker chains at 298 K. The big differences with the TB-SMA results are not surprising in view of the earlier comparisons. As far as we know, the effect of temperature on the mechanical behavior of gold nanowire has not been reported in experiments.

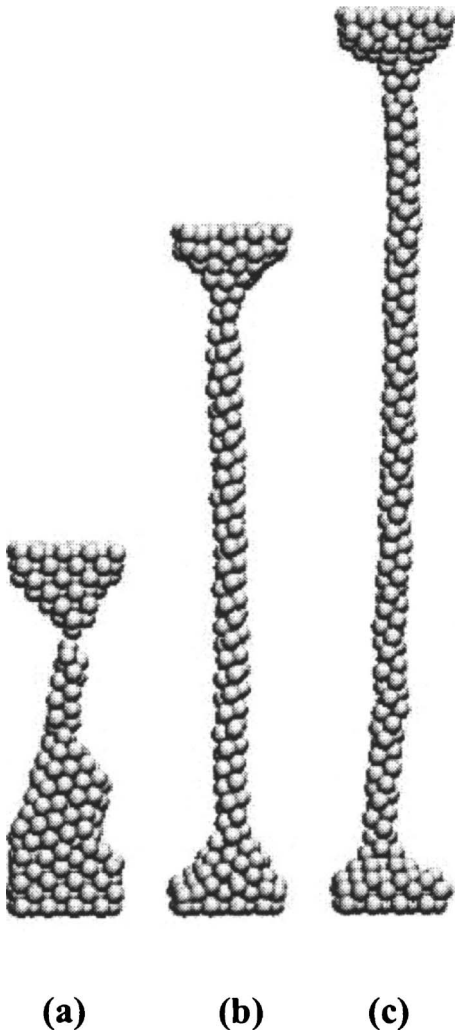

FIG. 4. The snapshots of the break-junction structures for small Au (001) system at 298 K given by the three force fields: (a) the TB-SMA result (2300 ps), (b) the glue model result (7080 ps), and (c) the EAM result (10 320 ps).

It should be noted that there are limits on the range of validity of TB-SMA. For example, TB-SMA does not predict planar structures for very small gold clusters[47,48] in which the coordination numbers of all the Au atoms are extremely small. For the system sizes of this work, however, the validity of TB-SMA potential in the generations of monatomic gold chains is confirmed through the comparison with the higher-level DFT method.

Finally, we demonstrate that the TB-SMA potential can properly predict the force needed to break a gold monatomic chain. The definition of tensile force is in line with the work of Rubio-Bollinger *et al.*[30] and is calculated based on the total forces exerted on the top two rigid layers of gold atoms. Figure 5 shows the sawtooth variation of the tensile force applied along the monatomic chain direction versus the elon-

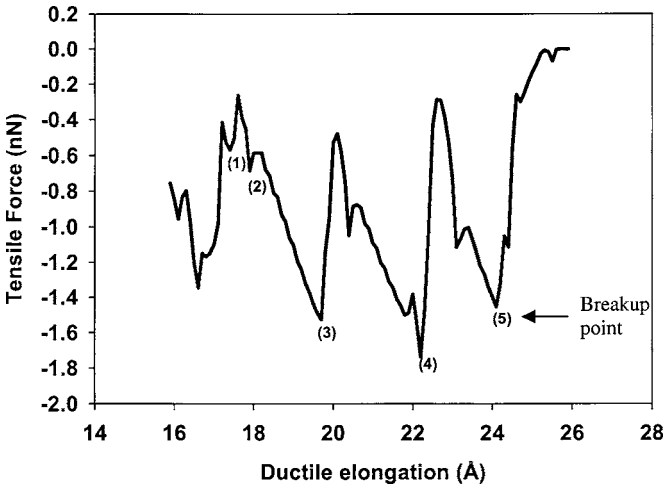

FIG. 5. The variations of the tensile force as a function of the elongation length predicted by the TB-SMA potential, starting at the formation of monatomic chains. The atomic system corresponds to the large Au (001) system at 0.01 K (Fig. 2). The numbers (1) to (5) represent the occurrence of one to five gold atoms in monatomic chains.

gation length for the large Au system [see configuration in Fig. 2(a)]. In the stages with a linearly growing tensile force the nanowire is elastically stretched with accumulation of elastic energy, while at the force jumps, abrupt atomic rearrangement occurs and the accumulated strain energy is released. Some of the force jumps correspond to the incorporation of an extra gold atom into the bridging atomic chain while other jumps originate from atomic rearrangements occurring in the region close to the chain. The tensile force is recorded after each relaxation is completed. The numbers (1) to (5) in Fig. 5 mark the occurrence of one to five monatomic atoms in the break junction. We find that the incorporation of new atoms in the break junction corresponds to the large jumps of tensile force in our simulation. Just before the breakup, the calculated tensile force is around 1.5 nN, as shown in Fig. 5, which is in good agreement with the STM experimental result (1.5±0.3 nN).[30]

IV. CONCLUSIONS

We have performed MD simulations combined with DFT energy calculations to investigate the mechanical elongation behavior of finite gold nanowires. The DFT energy calculations verify that among the three typical semiempirical potentials (i.e., the glue model, the EAM, and the TB-SMA potentials), the TB-SMA potential is the most suitable force field to describe the structural and mechanical properties of gold nanowires during elongation. Using the TB-SMA potential, we find that the elongation of gold nanowires leads to the formation of monatomic chains, as observed by many experiments. The less ductility predicted by TB-SMA at elevated temperature is in contrast to the predictions by the glue and EAM potentials. Currently, the dynamic elongations of Au nanowires with different sizes, along different crystal orientations, and immersed in different organic solvents using the TB-SMA potential are under extensive investigations.

ACKNOWLEDGMENTS

This work was supported by the Office of Science of the U.S. Department of Energy Computational Nanoscience project and by the Vanderbilt Advanced Computing Center for Research and Education (ACCRE). Parts of the calculations were performed at the Center for Computational Sciences at Oak Ridge National Laboratory (ORNL).

[1] X. D. Cui, A. Primak, X. Zarate, J. Tomfohr, O. F. Sankey, A. L. Moore, T. A. Moore, D. Gust, G. Harris, and S. M. Lindsay, Science **294**, 571 (2001).
[2] M. A. Reed, C. Zhou, C. J. Muller, T. P. Burgin, and J. M. Tour, Science **278**, 252 (1997).
[3] B. Q. Xu and N. J. J. Tao, Science **301**, 1221 (2003).
[4] M. Di Ventra, S. T. Pantelides, and N. D. Lang, Phys. Rev. Lett. **84**, 979 (2000).
[5] P. E. Kornilovitch and A. M. Bratkovsky, Phys. Rev. B **64**, 195413 (2001).
[6] P. S. Krstic, D. J. Dean, X. G. Zhang, D. Keffer, Y. S. Leng, P. T. Cummings, and J. C. Wells, Comput. Mater. Sci. **28**, 321 (2003).
[7] J. M. Seminario, A. G. Zacarias, and J. M. Tour, J. Phys. Chem. A **103**, 7883 (1999).
[8] K. Stokbro, J. Taylor, M. Brandbyge, J. L. Mozos, and P. Ordejon, Comput. Mater. Sci. **27**, 151 (2003).
[9] J. I. Pascual, J. Mendez, J. Gomezherrero, A. M. Baro, N. Garcia, and V. T. Binh, Phys. Rev. Lett. **71**, 1852 (1993).
[10] A. I. Yanson, G. R. Bollinger, H. E. van den Brom, N. Agrait, and J. M. van Ruitenbeek, Nature (London) **395**, 783 (1998).
[11] H. Ohnishi, Y. Kondo, and K. Takayanagi, Nature (London) **395**, 780 (1998).
[12] G. Rubio, N. Agrait, and S. Vieira, Phys. Rev. Lett. **76**, 2302 (1996).
[13] P. E. Marszalek, W. J. Greenleaf, H. B. Li, A. F. Oberhauser, and J. M. Fernandez, Proc. Natl. Acad. Sci. U.S.A. **97**, 6282 (2000).
[14] J. M. Krans, J. M. Vanruitenbeek, V. V. Fisun, I. K. Yanson, and L. J. Dejongh, Nature (London) **375**, 767 (1995).
[15] C. J. Muller, J. M. Vanruitenbeek, and L. J. Dejongh, Phys. Rev. Lett. **69**, 140 (1992).
[16] V. Rodrigues, T. Fuhrer, and D. Ugarte, Phys. Rev. Lett. **85**, 4124 (2000).
[17] P. Z. Coura, S. B. Legoas, A. S. Moreira, F. Sato, V. Rodrigues, S. O. Dantas, D. Ugarte, and D. S. Galvao, Nano Lett. **4**, 1187 (2004).
[18] V. Rodrigues and D. Ugarte, Phys. Rev. B **63**, 073405 (2001).
[19] R. N. Barnett and U. Landman, Nature (London) **387**, 788 (1997).
[20] E. Z. da Silva, A. J. R. da Silva, and A. Fazzio, Phys. Rev. Lett. **87**, 256102 (2001).
[21] M. R. Sorensen, M. Brandbyge, and K. W. Jacobsen, Phys. Rev. B **57**, 3283 (1998).
[22] G. Bilalbegovic, J. Phys.: Condens. Matter **13**, 11531 (2001).
[23] G. M. Finbow, R. M. LyndenBell, and I. R. McDonald, Mol. Phys. **92**, 705 (1997).
[24] U. Landman, W. D. Luedtke, B. E. Salisbury, and R. L. Whetten, Phys. Rev. Lett. **77**, 1362 (1996).
[25] F. Cleri and V. Rosato, Phys. Rev. B **48**, 22 (1993).
[26] T. N. Todorov and A. P. Sutton, Phys. Rev. Lett. **70**, 2138 (1993).
[27] T. N. Todorov and A. P. Sutton, Phys. Rev. B **54**, 14234 (1996).
[28] H. Hakkinen, R. N. Barnett, A. G. Scherbakov, and U. Landman, J. Phys. Chem. B **104**, 9063 (2000).
[29] D. Kruger, H. Fuchs, R. Rousseau, D. Marx, and M. Parrinello, Phys. Rev. Lett. **89**, 186402 (2002).
[30] G. Rubio-Bollinger, S. R. Bahn, N. Agrait, K. W. Jacobsen, and S. Vieira, Phys. Rev. Lett. **87**, 026101 (2001).
[31] E. Tosatti, S. Prestipino, S. Kostlmeier, A. Dal Corso, and F. D. Di Tolla, Science **291**, 288 (2001).
[32] F. Ercolessi, M. Parrinello, and E. Tosatti, Philos. Mag. A **58**, 213 (1988).
[33] A. F. Voter, *Los Alamos Unclassified Technical Report No.* LA-UR 93-3901, 1993 (unpublished).
[34] H. Mehrez and S. Ciraci, Phys. Rev. B **56**, 12632 (1997).
[35] H. S. Park and J. A. Zimmerman, Phys. Rev. B **72**, 054106 (2005).
[36] M. S. Daw and M. I. Baskes, Phys. Rev. B **29**, 6443 (1984).
[37] G. J. Martyna, M. E. Tuckerman, D. J. Tobias, and M. L. Klein, Mol. Phys. **87**, 1117 (1996).
[38] S. Nose, J. Chem. Phys. **81**, 511 (1984).

[39] M. Tuckerman, B. J. Berne, and G. J. Martyna, J. Chem. Phys. **97**, 1990 (1992).
[40] J. P. Perdew and A. Zunger, Phys. Rev. B **23**, 5048 (1981).
[41] D. Vanderbilt, Phys. Rev. B **41**, 7892 (1990).
[42] G. Kresse and J. Furthmuller, Phys. Rev. B **54**, 11169 (1996).
[43] I. Galanakis, N. Papanikolaou, and P. H. Dederichs, Surf. Sci. **511**, 1 (2002).
[44] B. D. Yu and M. Scheffler, Phys. Rev. B **56**, R15569 (1997).
[45] Q. Pu, Y. S. Leng, and P. T. Cummings (unpublished).
[46] J. W. Kang and H. J. Hwang, Nanotechnology **13**, 503 (2002).
[47] H. Hakkinen, M. Moseler, and U. Landman, Phys. Rev. Lett. **89**, 033401 (2002).
[48] L. Xiao, B. Tollberg, X. K. Hu, and L. C. Wang, J. Chem. Phys. **124**, 114309 (2006).